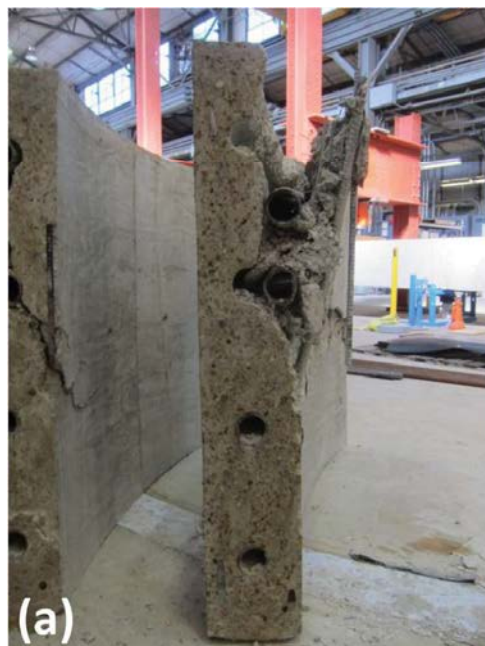


V. 114, NO. 4
JULY-AUGUST 2017

ACI STRUCTURAL JOURNAL

A JOURNAL OF THE AMERICAN CONCRETE INSTITUTE



American Concrete Institute

Board of Direction

President

Khaled Awad

Vice Presidents

David A. Lange
Randall W. Poston

Directors

JoAnn P. Browning
Cesar A. Constantino
Frances T. Griffith
H. R. Trey Hamilton
R. Doug Hooton
Joe Hug
Kimberly Kayler
William M. Klorman
Neven Krstulovic-Opara
Tracy D. Marcotte
Antonio Nanni
Roberto Stark

Past President Board Members

Michael J. Schneider
Sharon L. Wood
William E. Rushing Jr.

Executive Vice President

Ron Burg

Technical Activities Committee

H. R. Trey Hamilton, Chair
Michael C. Brown
JoAnn P. Browning
Catherine E. French
Harry A. Gleich
Fred R. Goodwin
Larry Kahn
Neven Krstulovic-Opara
Kimberly Kurtis
Tracy D. Marcotte
Michael Stenko
Bruce A. Suprenant
Andrew W. Taylor

Staff

Publisher
John C. Glumb

Engineering

Managing Director
Michael L. Tholen

Managing Editor

Jerzy Z. Zemajtis

Staff Engineers

Katie A. Amelio
Robert M. Howell
Khaled Nahlawi
Marc M. Rached
Matthew R. Senecal
Steve S. Szoke
Gregory M. Zeisler

Publishing Services

Manager
Barry M. Bergin

Editors

Carl R. Bischof
Tiesha Elam
Kaitlyn J. Hinman
Kelli R. Slayden

Editorial Assistant

Angela R. Matthews



ACI STRUCTURAL JOURNAL

JULY-AUGUST 2017, V. 114, No. 4

A JOURNAL OF THE AMERICAN CONCRETE INSTITUTE
AN INTERNATIONAL TECHNICAL SOCIETY

- 795 Elongation Tolerance for Short Tendons in Post-Tensioned Building Structures**, by Carol Hayek and Thomas H.-K. Kang
- 803 Shear Design Considering Interaction between Steel Stirrups and Carbon Fiber-Reinforced Polymer Strips**, by Yungon Kim, Wassim M. Ghannoum, and James O. Jirsa
- 815 Behavior of Steel Fiber-Reinforced High-Strength Concrete Columns under Different Loads**, by Muhammad N. S. Hadi, Emdad K. Z. Balanji, and M. Neaz Sheikh
- 827 Shear Strength of Concrete Composite Beams with Shear Reinforcements**, by Chul-Goo Kim, Hong-Gun Park, Geon-Ho Hong, Su-Min Kang, and Hyerin Lee
- 839 Nonuniform Bond Stress Distribution Model for Evaluation of Bar Development Length**, by Hyeon-Jong Hwang, Hong-Gun Park, and Wei-Jian Yi
- 851 Effect of Steel Fiber for Crack Control in Concrete Slabs with Steel Deck Plates**, by Hyeon-Jong Hwang, Hong-Gun Park, Geon-Ho Hong, Gap-Deug Kim, and Se-Jin Choi
- 861 Externally Bonded Reinforcement on Grooves Technique in Circular Reinforced Columns Strengthened with Longitudinal Carbon Fiber-Reinforced Polymer under Eccentric Loading**, by Ala Torabian and Davood Mostofinejad
- 875 Size Effect on Punching Strength of Reinforced Concrete Slabs with and without Shear Reinforcement**, by Abdullah Dönmez and Zdeněk P. Bažant
- 887 Effectiveness of High-Strength Hoops in High-Strength Flexural Members**, by Leonardus S. B. Wibowo, Min-Yuan Cheng, Feng-Cheng Huang, and Ting-Yu Tai
- 899 Reinforced Concrete One-Way Slabs with Large Steps**, by Thomas H.-K. Kang, Sanghee Kim, Seongwon Hong, Geon-Ho Hong, and Hong-Gun Park
- 911 Evaluation of Impact Resistance of Steel Fiber-Reinforced Concrete Panels Using Design Equations**, by Sanghee Kim, Thomas H.-K. Kang, and Hyun Do Yun
- 923 Effect of High-Strength Materials on Lateral Strength of Stocky Reinforced Concrete Walls**, by Steven M. Barbachyn, Robert D. Devine, Ashley P. Thrall, and Yahya C. Kurama

Contents cont. on next page

Discussion is welcomed for all materials published in this issue and will appear ten months from this journal's date if the discussion is received within four months of the paper's print publication. Discussion of material received after specified dates will be considered individually for publication or private response. ACI Standards published in ACI Journals for public comment have discussion due dates printed with the Standard.

ACI Structural Journal

Copyright © 2017 American Concrete Institute. Printed in the United States of America.

The *ACI Structural Journal* (ISSN 0889-3241) is published bimonthly by the American Concrete Institute. Publication office: 38800 Country Club Drive, Farmington Hills, MI 48331. Periodicals postage paid at Farmington, MI, and at additional mailing offices. Subscription rates: \$168 per year (U.S. and possessions), \$177 (elsewhere), payable in advance. POSTMASTER: Send address changes to: *ACI Structural Journal*, 38800 Country Club Drive, Farmington Hills, MI 48331.

Canadian GST: R 1226213149.

Direct correspondence to 38800 Country Club Drive, Farmington Hills, MI 48331. Telephone: +1,248,848,3700. Facsimile (FAX): +1,248,848,3701. Website: <http://www.concrete.org>.

CONTENTS

- 937 **Effect of Column Size and Reinforcement Ratio on Shear Strength of Glass Fiber-Reinforced Polymer Reinforced Concrete Two-Way Slabs**, by Mohamed Hassan, Amir Fam, Brahim Benmokrane, and Emmanuel Ferrier
- 951 **Sustained Load Performance of Adhesive Anchor Systems in Concrete**, by Todd M. Davis and Ronald A. Cook
- 959 **Health Study of Reinforced Concrete Test Bridge with Pier Damage**, by Steven B. Worley and Elizabeth K. Ervin
- 969 **Cyclic Loading Test for Walls of Aspect Ratio 1.0 and 0.5 with Grade 550 MPa (80 ksi) Shear Reinforcing Bars**, by Jang-Woon Baek, Hong-Gun Park, Jae-Hoon Lee, and Chang-Joon Bang
- 983 **Behavior of Curved Post-Tensioned Concrete Structures without Through-Thickness Reinforcement**, by Jongkwon Choi, Clint R. Woods, Trevor D. Hrynyk, and Oguzhan Bayrak
- 995 **Influence of Width-to-Effective Depth Ratio on Shear Strength of Reinforced Concrete Elements without Web Reinforcement**, by Antonio Conforti, Fausto Minelli, and Giovanni A. Plizzari
- 1007 **Shear Strength of Reinforced Limestone Aggregate Concrete Beams**, by Kenichiro Nakarai, Yuko Ogawa, Kenji Kawai, and Ryoichi Sato
- 1019 **Shear Behavior of Squat Heavyweight Concrete Shear Walls with Construction Joints**, by Ju-Hyun Mun, Keun-Hyeok Yang, and Jin-Kyu Song
- 1031 **Beam Experiments on Acceptance Criteria for Bridge Load Tests**, by Eva O. L. Lantsoght, Yuguang Yang, Cor van der Veen, Ane de Boer, and Dick A. Hordijk
- 1043 **Interface Model for Bond-Slip and Dowel-Action Behavior**, by Alexandra Kottari, Marios Mavros, Juan Murcia-Delso, and P. Benson Shing
- 1055 **Reinforced Concrete Shear Design: Shortcomings and Remedy**, by Michael D. Kotsovos
- 1067 **Discussion**
- Serviceability and Ultimate Load Behavior of Concrete Beams Reinforced with Basalt Fiber-Reinforced Polymer Bars**. Paper by Thilana Ovitigala, Mustapha A. Ibrahim, and Mohsen A. Issa

UPCOMING ACI CONVENTIONS

The following is a list of scheduled ACI conventions:

2017—October 15-19, Disneyland Hotel, Anaheim, CA

2018—March 25-29, Grand America & Little America, Salt Lake City, UT

2018—October 14-18, Rio All-Suites Hotel & Casino, Las Vegas, NV

For additional information, contact:

Event Services, ACI
38800 Country Club Drive, Farmington Hills, MI 48331
Telephone: +1.248.848.3795
e-mail: conventions@concrete.org

ON COVER: 114-S81, p. 990, Fig. 9—Typical sectional crack pattern: (a) Specimen 1 at 15-degree location; and (b) Specimen 2 at 8-degree location.

Permission is granted by the American Concrete Institute for libraries and other users registered with the Copyright Clearance Center (CCC) to photocopy any article contained herein for a fee of \$3.00 per copy of the article. Payments should be sent directly to the Copyright Clearance Center, 21 Congress Street, Salem, MA 01970. ISSN 0889-3241/98 \$3.00. Copying done for other than personal or internal reference use without the express written permission of the American Concrete Institute is prohibited. Requests for special permission or bulk copying should be addressed to the Managing Editor, *ACI Structural Journal*, American Concrete Institute.

The Institute is not responsible for statements or opinions expressed in its publications. Institute publications are not able to, nor intend to, supplant individual training, responsibility, or judgment of the user, or the supplier, of the information presented.

Papers appearing in the *ACI Structural Journal* are reviewed according to the Institute's Publication Policy by individuals expert in the subject area of the papers.

Contributions to *ACI Structural Journal*

The *ACI Structural Journal* is an open forum on concrete technology and papers related to this field are always welcome. All material submitted for possible publication must meet the requirements of the "American Concrete Institute Publication Policy" and "Author Guidelines and Submission Procedures." Prospective authors should request a copy of the Policy and Guidelines from ACI or visit ACI's website at www.concrete.org prior to submitting contributions.

Papers reporting research must include a statement indicating the significance of the research.

The Institute reserves the right to return, without review, contributions not meeting the requirements of the Publication Policy.

All materials conforming to the Policy requirements will be reviewed for editorial quality and technical content, and every effort will be made to put all acceptable papers into the information channel. However, potentially good papers may be returned to authors when it is not possible to publish them in a reasonable time.

Discussion

All technical material appearing in the *ACI Structural Journal* may be discussed. If the deadline indicated on the contents page is observed, discussion can appear in the designated issue. Discussion should be complete and ready for publication, including finished, reproducible illustrations. Discussion must be confined to the scope of the paper and meet the ACI Publication Policy.

Follow the style of the current issue. Be brief—1800 words of double spaced, typewritten copy, including illustrations and tables, is maximum. Count illustrations and tables as 300 words each and submit them on individual sheets. As an approximation, 1 page of text is about 300 words. Submit one original typescript on 8-1/2 x 11 plain white paper, use 1 in. margins, and include two good quality copies of the entire discussion. References should be complete. Do not repeat references cited in original paper; cite them by original number. Closures responding to a single discussion should not exceed 1800-word equivalents in length, and to multiple discussions, approximately one half of the combined lengths of all discussions. Closures are published together with the discussions.

Discuss the paper, not some new or outside work on the same subject. Use references wherever possible instead of repeating available information.

Discussion offered for publication should offer some benefit to the general reader. Discussion which does not meet this requirement will be returned or referred to the author for private reply.

Send manuscripts to:
<http://mc.manuscriptcentral.com/acj>

Send discussions to:
Journals.Manuscripts@concrete.org

Title No. 114-S72

Effectiveness of High-Strength Hoops in High-Strength Flexural Members

by Leonardus S. B. Wibowo, Min-Yuan Cheng, Feng-Cheng Huang, and Ting-Yu Tai

This paper evaluates cyclic behavior of reinforced concrete (RC) flexural members using high-strength steel and concrete materials. The specified yield strength (f_y) of high-strength longitudinal and transverse reinforcement used in this study is 100 and 115 ksi (690 and 785 MPa), respectively. A total of 10 specimens were tested under displacement reversals. The primary test parameters were the ratio between transverse reinforcement spacing and longitudinal bar diameter (s/d_b ratio), hoop configuration, and specimen-normalized shear demands. Test results showed that all specimens achieved flexural capacity before failure initiated by buckling of longitudinal reinforcement. Among the three hoop configurations investigated in this study, specimens with welded one-piece close hoops exhibited the largest deformation capacity with all other conditions being equal to each other. A usable shear strength between 54 and 120 ksi (375 and 827 MPa) was observed in the specimens using high-strength transverse reinforcement. A maximum s/d_b of 6 appears to be acceptable for the high-strength longitudinal reinforcement in specimens with shear demand of $3.5\sqrt{f'_c}$ (psi) ($0.29\sqrt{f'_c}$ [MPa]) or less. Those specimens exhibited a minimum drift capacity of 4.8%. For specimens with shear demand of approximately $5.5\sqrt{f'_c}$ (psi) ($0.46\sqrt{f'_c}$ [MPa]), a minimum deformation capacity of 3.5% drift can be achieved by limiting the s/d_b to less than 5.

Keywords: cyclic; deformation capacity; high-strength; hoop; strength; USD685; USD785.

INTRODUCTION

The potential of using high-strength steel with specified yield strength f_y approximately 100 ksi (690 MPa) as the primary longitudinal reinforcement has been evaluated previously (Falkner et al. 2008; Rautenberg 2011; Cheng and Giduquio 2014; Tavallali et al. 2014). Test results indicate that specimens reinforced with high-strength longitudinal steel exhibited comparable responses in terms of strength and deformation as specimens reinforced with conventional Grade 60 longitudinal steel, providing that transverse reinforcement was adequately spaced. However, it is not clear in regard to transverse reinforcement whether the maximum s/d_b ratio specified in the current ACI 318-05 (ACI Committee 318 2005) for buckling resistance of Grade 60 longitudinal reinforcement is applicable to longitudinal reinforcement with yield strength of 100 ksi (690 MPa) or higher (in which the s/d_b ratio is defined as the spacing of the transverse reinforcement divided by the diameter of the smallest longitudinal reinforcement).

For beam specimens subjected to monotonic gravity-type loading, test results by Giduquio et al. (2015) suggest a maximum s/d_b of 8 to resist buckling of longitudinal reinforcement with $f_y = 100$ ksi (690 MPa). For members subjected to earthquake-type loading, a maximum s/d_b of 4

is recommended for Grade 100 ($f_y = 100$ ksi [690 MPa]) and Grade 120 ($f_y = 120$ ksi [827 MPa]) longitudinal reinforcement in NIST GCR 14-917-30 (2014). This suggestion is derived based on analytical approaches without considering stiffness and strength of the transverse reinforcement and, as indicated by the report, further tests are needed to verify this value. Providing Grade 60 transverse reinforcement with a s/d_b of 8, test results (Cheng and Giduquio 2014) show that specimens using longitudinal reinforcement with f_y exceeding 100 ksi (690 MPa) were able to sustain the displacement reversals to 4% drift. In this study, specimen shear demand was relative low at approximately $2\sqrt{f'_c}$ (psi) or $0.17\sqrt{f'_c}$ (MPa).

The idea of using high-strength steel as shear reinforcement in reinforced concrete (RC) flexural members has been also studied previously. Test results of nine beam specimens (Sumpter et al. 2009) suggest that ACI 318-14 (ACI Committee 318 2014) can be conservatively applied to the design of high-strength stirrups using a yield strength of 80 ksi (552 MPa)—that is, 20 ksi (138 MPa) higher than the current code limit but less than the stirrup tested yield strength. Lee et al. (2011), through tests of 32 beam specimens, observed that those reinforced with high-strength stirrups failed after reaching stirrup yielding strain corresponding to yield stress over 100 ksi (690 MPa). Test specimens in both aforementioned studies were reinforced with a one-piece closed stirrup, as shown in Fig. 1(a) and subjected to monotonic gravity-type loading. Experimental data for flexural members using high-strength transverse reinforcement under cyclic loading is relatively limited. ACI 318-14 (ACI Committee 318 2014) permits the use of a two-piece closed hoop in RC flexural members, as shown in Fig. 1(b). However, experimental evidence to support this hoop configuration is not well documented according to the authors' knowledge. The two-piece closed stirrup is widely used in practice because of easy installation.

This research aims to study cyclic behavior of RC flexural members using high-strength steel and concrete materials. A total of 10 beam specimens were tested under displacement reversals. Primary test variables are: 1) s/d_b ; 2) hoop configurations; and 3) specimen normalized shear demands. Three hoop configurations are investigated: a one-piece closed hoop with standard seismic hooks, as shown in Fig. 1(a); a two-piece stirrup including a U-shape stirrup and a cap

ACI Structural Journal, V. 114, No. 4, July-August 2017.

MS No. S-2016-077.R1, doi: 10.14359/51689620, received September, 29, 2016, and reviewed under Institute publication policies. Copyright © 2017, American Concrete Institute. All rights reserved, including the making of copies unless permission is obtained from the copyright proprietors. Pertinent discussion including author's closure, if any, will be published ten months from this journal's date if the discussion is received within four months of the paper's print publication.

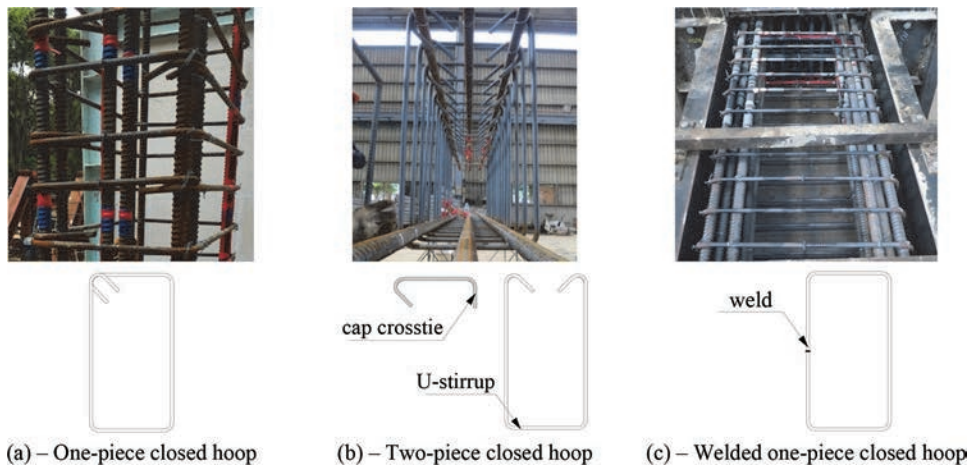


Fig. 1—Hoop configuration.

Table 1—Required material properties of reinforcement

Bar type	Minimum ϵ_{shs} , [*] %	Minimum ϵ_{stl} , [†] %	Minimum f_y , [‡] ksi (MPa)	Minimum f_u , [§] ksi (MPa)
USD685	1.4	10	100 (690)	$>1.25f_y$
USD785	NA	8	115 (785)	135 (930)

^{*} ϵ_{sh} is strain at onset of strain hardening.

[†] ϵ_{stl} is total fracture elongation, measured within an 8 in. (200 mm) gauge length.

[‡] f_y is yield strength determined using 0.2% offset method.

[§] f_u is tensile strength.

cross tie, as shown in Fig. 1(b); and a welded one-piece closed hoop provided by a Japanese steel manufacturer, as shown in Fig. 1(c). Through test results, the maximum s/d_b ratio for buckling restraint of the high-strength longitudinal reinforcement and maximum usable stress of high-strength transverse reinforcement for shear resistance are discussed.

The high-strength longitudinal and transverse reinforcement used in the test specimens comply with Japanese USD685 and USD785 steel properties, respectively (Aoyama 2001). The required material properties of USD685 and USD785 high-strength steels are summarized in Table 1. The high-strength concrete used in this study refers to concrete strength, f'_c , exceeding 10 ksi (69 MPa).

RESEARCH SIGNIFICANCE

An experimental program consisting of 10 beam specimens is conducted to investigate effectiveness of transverse reinforcement in high-strength RC flexural members subjected to cyclic displacement reversals. The maximum s/d_b for buckling resistance and maximum steel stress that can be used for shear resistance are discussed. Test results provide valuable information for the development of future building codes.

TEST SPECIMEN

The key design parameters of all test specimens are presented in Table 2. Specimen geometry and reinforcement layout are illustrated in Fig. 2. All test specimens have an identical cross section of 16 x 28 in. (400 x 700 mm) and a clear height of 71 in. (1800 mm). The first hoop is placed 2 in. (50 mm) away from the concrete base block. Design parameters listed in Table 2 are determined according to

specified material properties. Shear stress demand v_u is evaluated based on nominal flexural strength M_n of the specimen. Nominal flexural strength, in turn, is determined using stress block per the ACI 318-14 for concrete and elastic-plastic stress-strain relationship for USD685 high-strength steel.

Specimens are labeled in three segments that are connected by hyphens. From left to right, the label is led by description of concrete strength, followed by number of longitudinal reinforcement, and ended by description of transverse reinforcement. Concrete is classified by either HC or RC for strength, f'_c greater or less than 10 ksi (69 MPa), respectively. Among all test specimens, only one specimen was designed with concrete with f'_c less than 10 ksi (69 MPa). The longitudinal reinforcement arrangements are either 6 No. 10 (D32), 12 No. 10 (D32), or 12 No. 8 (D25), each corresponding to the label 6#10, 12#10 and 12#8, respectively. USD685 high-strength steel is used as the longitudinal reinforcement in all test specimens.

No. 4 (D13) transverse reinforcement is used in all specimens but with different strengths, spacing and configurations. The descriptor for transverse reinforcement starts with steel strength—H refers to the use of high-strength USD785 steel and C refers to the use of conventional Grade 60 steel. Among all test specimens, only one specimen was designed with Grade 60 transverse reinforcement. After steel strength, the description continues with hoop spacing expressed in terms of the diameter of smallest longitudinal reinforcement. Finally, the description ends with hoop configuration—W for the welded one-piece close hoop and T for the two-piece closed hoop. No letter is assigned for the one-piece closed hoop configuration. For both one- and two-piece closed hoops, the orientation of the 135-degree seismic hook alternated along the height of the specimen, as shown in Fig. 1(a) and 1(b). For the welded closed hoop, the welding point was also altered left and right along the height of the specimen, Fig. 1(c). Both 90- and 135-degree hooks were fabricated to satisfy minimum inside bend diameter and minimum straight extension per ACI 318-14. A concrete clear cover of 1.2 in. (30 mm) was provided for all test specimens.

TEST SETUP

The test setup is presented in Fig. 3. All specimens were tested in a vertical position. The concrete base block was

Table 2—Specimen design parameters

Specimen label	Specified material properties			s/d_b	Hoop configuration	v_u^* psi (MPa)
	f_c' , ksi (MPa)	f_y , ksi (MPa)	f_{yt} , ksi (MPa)			
HC_6#10_H4d _b	10 (69)	100 (690)	115 (785)	3.7	One-piece closed hoop	2.66 (0.22)
HC_12#10_H4d _b	10 (69)	100 (690)	115 (785)	3.7	One-piece closed hoop	5.11 (0.43)
HC_12#10_H4d _b T	10 (69)	100 (690)	115 (785)	3.7	Two-piece closed hoop	5.11 (0.43)
HC_12#10_C3d _b T	10 (69)	100 (690)	60 (414)	2.8	Two-piece closed hoop	5.11 (0.43)
HC_12#10_H4d _b W	10 (69)	100 (690)	115 (785)	3.7	Welded one-piece	5.11 (0.43)
RC_12#10_H4d _b	5 (34.5)	100 (690)	115 (785)	3.7	One-piece closed hoop	6.89 (0.57)
HC_12#10_H5d _b	10 (69)	100 (690)	115 (785)	4.7	One-piece closed hoop	5.11 (0.43)
HC_12#8_H6d _b	10 (69)	100 (690)	115 (785)	6.0	One-piece closed hoop	3.39 (0.28)
HC_12#8_H5d _b	10 (69)	100 (690)	115 (785)	5.0	One-piece closed hoop	3.39 (0.28)
HC_12#8_H4d _b	10 (69)	100 (690)	115 (785)	4.0	One-piece closed hoop	3.39 (0.28)

* $v_u = \frac{M_n/a}{\sqrt{f_c'bd}}$, M_n , and f_c' are specified material strength.

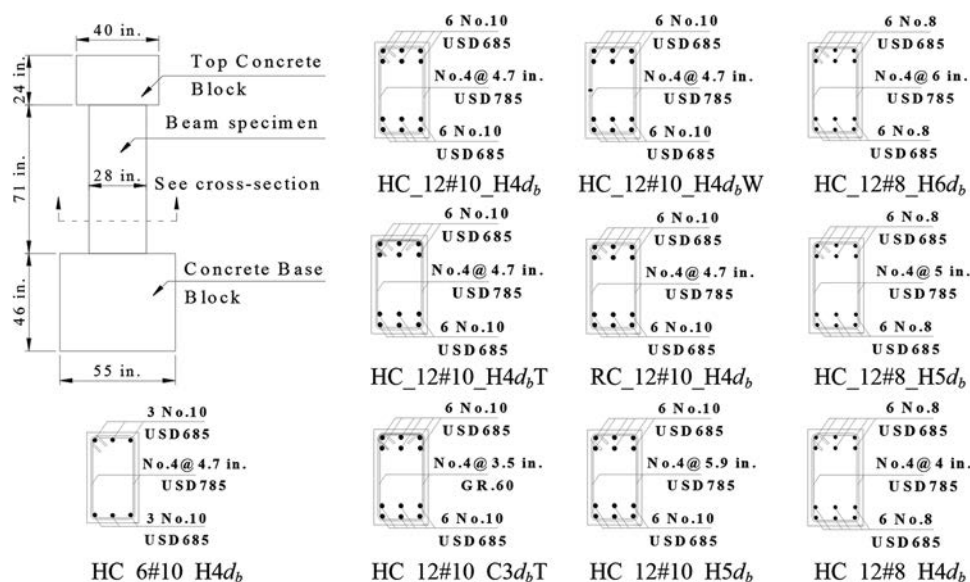


Fig. 2—Specimen geometry and reinforcement layout. (Note: 1 in. = 25.4 mm.)

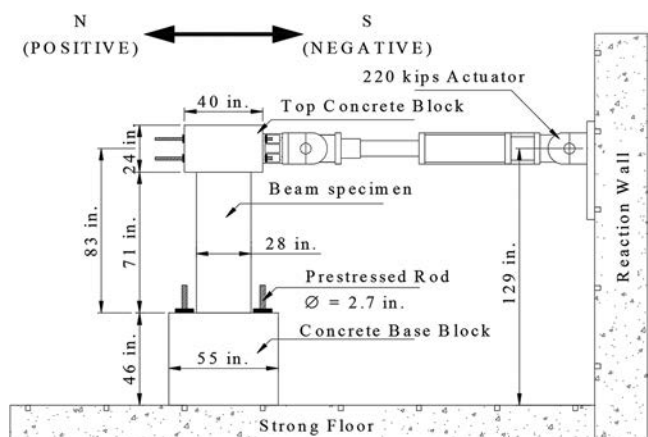


Fig. 3—Test setup. (Note: 1 in. = 25.4 mm.)

ties to the strong floor using four 2.7 in. (69 mm) diameter prestressed rods to simulate a fixed boundary condition. Lateral displacement reversals were applied to the center of

the top concrete block. Two ±220 kip (±100 tonf) actuators were used for load application. The shear span, measured from the center of load application to the top of the concrete base block, was 83 in. (2100 mm) resulting in a shear span-to-member effective depth ratio (a/d) of approximately 3.3 for specimens with six No. 10 longitudinal reinforcement, and 3.5 for specimens with 12 No. 10 or 12 No. 8 longitudinal reinforcement. Both actuators were displacement-controlled with loading history shown in Fig. 4, where the “target drift” is defined as the actuator displacement divided by the shear span. Each drift level consists of three cycles and the positive direction refers to the loading to the north. The 135-degree seismic hook on the hoop, if present, was consistently placed on the north side of the test floor (Fig. 3).

INSTRUMENTATION

External deformation of the specimen was monitored using an optical system that continuously tracked three-dimensional movements of markers attached to the specimen

Table 3—Summary of concrete cylinder strength and reinforcement properties

Specimen label	Concrete cylinder	Longitudinal reinforcement			Transverse reinforcement		
	f_c' , ksi (MPa)	f_y , ksi (MPa)	f_u , ksi (MPa)	ϵ_{su} , %	f_{yt} , ksi (MPa)	f_{ut} , ksi (MPa)	ϵ_{su} , %
HC_6#10_H4d _b	12.6 (87.0)	99.9 (689)	134.1 (924)	15.0	124.8 (860)	154.8 (1068)	12.7
HC_12#10_H4d _b	11.1 (76.5)	102.6 (707)	137.5 (948)	12.7	128.5 (886)	158.8 (1095)	12.3
HC_12#10_H4d _b T	12.2 (84.0)	102.6 (707)	137.5 (948)	12.7	128.5 (886)	158.8 (1095)	12.3
HC_12#10_C3d _b T	10.9 (75.2)	99.9 (689)	134.1 (924)	15.0	66.1 (456)	95.9 (661)	24.7
HC_12#10_H4d _b W	11.0 (75.8)	102.6 (707)	137.5 (948)	12.7	125.8 (868)	158.8 (1095)	11.0
RC_12#10_H4d _b	7.8 (53.4)	101.1 (697)	130.7 (901)	12.5	126.0 (869)	152.0 (1048)	9.2
HC_12#10_H5d _b	10.5 (72.5)	101.1 (697)	130.7 (901)	12.5	126.0 (869)	152.0 (1048)	9.2
HC_12#8_H6d _b	11.8 (81.0)	105.8 (730)	135.7 (935)	10.6	126.0 (869)	152.0 (1048)	9.2
HC_12#8_H5d _b	11.8 (81.0)	105.8 (730)	135.7 (935)	10.6	126.0 (869)	152.0 (1048)	9.2
HC_12#8_H4d _b	10.5 (72.5)	105.8 (730)	135.7 (935)	10.6	126.0 (869)	152.0 (1048)	9.2

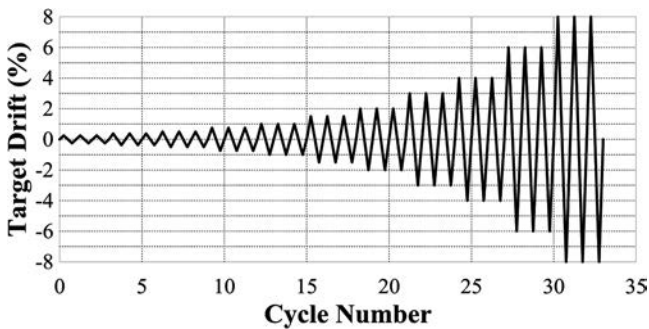


Fig. 4—Loading history.

surface. A total of 41 markers were used for each specimen: 36 were attached to the specimen in a 6 x 8 in. (15 x 200 mm) regular grid pattern and five were attached to the concrete base block to monitor support movement close to the top surface during the test. The positions of markers for the test specimen are depicted in Fig. 5. In addition, strain gauges were installed on longitudinal and transverse reinforcement at designated locations for each specimen.

TEST RESULTS

Materials

Specimens HC_6#10_H4d_b, HC_12#10_H4d_b, HC_12#10_H4d_bT, HC_12#10_H4d_bW, and HC_12#10_C3d_bT were each cast continuously with four concrete lifts from the same supplier. The coarse aggregate used in the concrete mixture was crushed river stone with a maximum size of 3/4 in. (19 mm). The rest of specimens were cast from another supplier with two concrete lifts (first to the top of concrete base block and then for the rest of the specimen). For those specimens, crushed granite with a maximum size of 1/2 in. (13 mm) was used as the coarse aggregate. Concrete compressive strength, as shown in Table 3, was determined based on the average compressive strength of at least six 4 x 8 in. (100 x 200 mm) cylinders that were tested within 10 days as the corresponding test specimen.

Direct tensile test was performed to evaluate stress-strain properties of longitudinal and transverse reinforcing. Some key values obtained from the average of three coupons are summarized in Table 3. The sample tensile test results

of USD685 and USD785 steels are presented in Fig. 6, where steel strain was measured using the optical system. Two markers with a gauge length of 8 in. (200 mm) were attached to the central part of steel coupon. Rupture strain ϵ_{su} is defined by the point corresponding to 10% force drop from the peak or the actual rupture point if 10% force drop is not available (ASTM A370 2012). Three additional coupon samples with welding points at the center were tested to confirm that the welding strength is greater than the material strength of USD785 steel.

General behavior

Hysteretic responses of all test specimens are presented in Fig. 7, where the target drift is defined as the lateral displacement measured from the top block divided by the shear span, and the modified drift is determined by deducting rotation and lateral displacement of the concrete base block from the target drift using recorded data from the markers. Unless specified as “target,” drift refers to the modified one hereafter in this paper. Numerical values of some key test results are summarized in Table 4. Ultimate drift ratio d_u is defined at the point when one of the following two criteria is first met: 1) the load dropped 20% from the peak on the envelope curve; or 2) the load dropped more than 20% in the repeated cycles at the same target drift level. Final states of all test specimens are presented in Fig. 8.

All specimens exhibited satisfactory hysteretic responses after completion of 3% target drift cycles. From 4% target drift to the end of the test, loud “bang” sounds were occasionally heard in all test specimens. Those bang sounds appeared to be caused by distress of transverse reinforcement that lost (partial/entire) anchorage provided by the seismic hooks. The bang sounds, typically accompanied by spalling of concrete cover, may lead to sudden loss of lateral resistance. For example, as can be seen from Fig. 7(a), lateral force of Specimen HC_6#10_H4d_b dropped suddenly at approximately -4% target drift with a very loud “bang” sound during the second cycle of 6% target drift. In addition to the sudden loss of lateral resistance, the legs of transverse reinforcement may pop out if the “bang” sounds were triggered by a loss of anchorage (Specimens HC_12#10_C3d_bT, RC_12#10_H4d_b, HC_12#10_H5d_b, and HC_12#8_H5d_b).

Table 4—Summary of test results

Specimen label	$V_{test}/\sqrt{f'_c}bd$, psi (MPa)	M_{test} , kip-ft (kN-m)	M_{test}/M_n	$M_{test}/M_{n, up}$	d_{us} , %	Usable shear strength ^a , ksi (MPa)
HC_6#10_H4d _b	2.81 (0.23)	865 (1173)	1.17	0.99	5.41	54.4 (375)
HC_12#10_H4d _b	5.43 (0.45)	1469 (1991)	1.08	0.94	3.53	83.9 (579)
HC_12#10_H4d _b T	5.12 (0.43)	1451 (1968)	1.06	0.92	3.47	63.3 (437)
HC_12#10_C3d _b T	5.49 (0.46)	1473 (1997)	1.11	0.94	4.55	76.6 (528)
HC_12#10_H4d _b W	5.50 (0.46)	1481 (2008)	1.09	0.95	5.56	102.9 (710)
RC_12#10_H4d _b	6.08 (0.51)	1375 (1865)	1.05	0.90	5.18	95.2 (657)
HC_12#10_H5d _b	5.26 (0.44)	1398 (1896)	1.04	0.90	5.02	120.0 (827)
HC_12#8_H6d _b	3.51 (0.29)	995 (1349)	1.06	0.95	4.84	87.0 (600)
HC_12#8_H5d _b	3.44 (0.28)	1001 (1357)	1.07	0.96	5.26	72.4 (499)
HC_12#8_H4d _b	3.48 (0.29)	999 (1354)	1.07	0.96	5.80	58.3 (402)

^aUsable shear strength is determined using average lateral force interpolated at ±3% drift for envelope of third loading cycle.

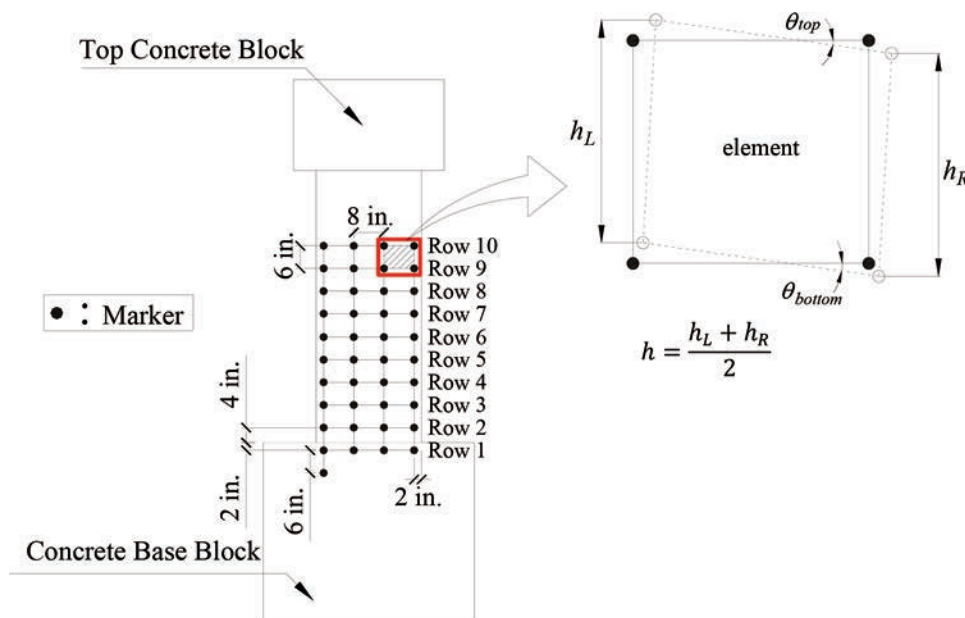


Fig. 5—Location of instrumentation for displacement measurement. (Note: 1 in. = 25.4 mm.)

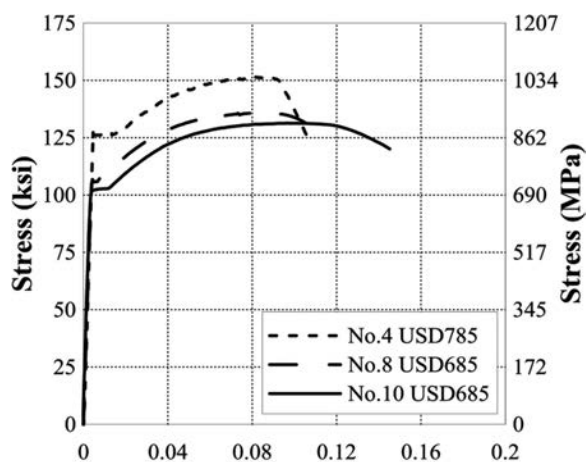


Fig. 6—Sample tensile properties of reinforcement.

For Specimens HC_6#10_H4d_b, HC_12#10_H4d_b, and HC_12#10_H4d_bT, severe spalling of concrete cover was observed during the 4% target drift cycles. For the rest of

the specimens, spalling of concrete cover was limited to the bottom corner after completion of the 4% target drift cycles and extensive loss of concrete cover was observed during the 6% target drift cycles. After extensive loss of concrete cover, as observed in all test specimens, the exposed longitudinal reinforcements on both sides buckled outward when subjected to compression. In addition, different numbers of seismic hooks for specimens using one-piece or two-piece closed hoops were gradually pushed out from their original 135-degree configuration to approximately 90 degrees at this stage. Some hooks lost all anchorage and the legs of transverse reinforcements popped out.

Three distinct behaviors were observed in cycles where specimens lost significant lateral resistance. Type 1: The major inclined crack widths increased rapidly. In this case, the specimen above the major inclined cracks appeared to move horizontally away from the lower part of the specimen. Type 2: The specimen appeared to slide horizontally along the base. And, Type 3, the specimen appeared to slide along a horizontal plane a certain distance away from the base. Typically, a layer of transverse reinforcement was provided on

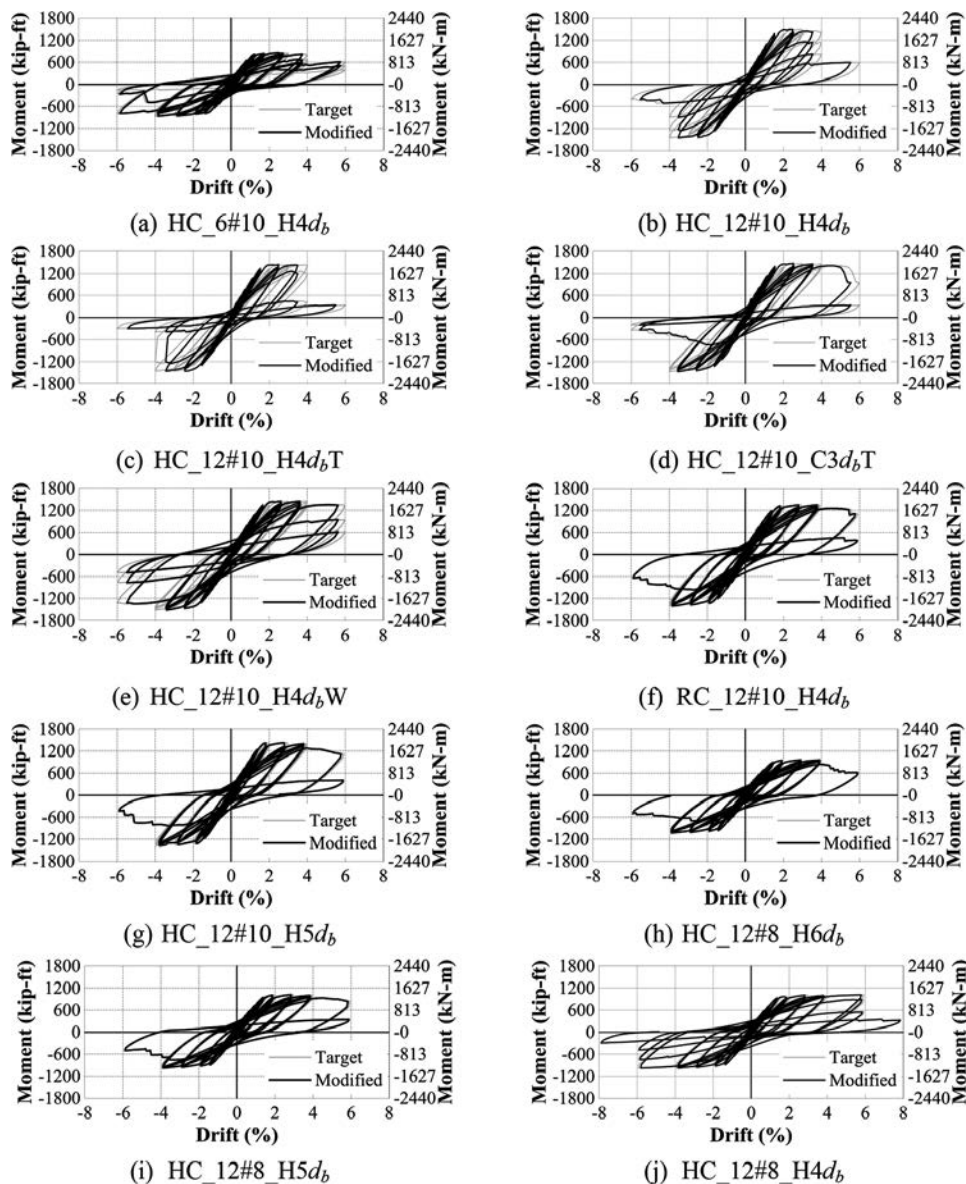


Fig. 7—Hysteretic response.

that plane. The observed behaviors in each specimen based on the aforementioned categories are summarized in Table 5. The schematic drawings along with photos taken from three specimens during the test are provided in Fig. 9 to illustrate the three distinct behaviors. While some specimens were dominated by one behavior, others exhibited a combination of different behaviors. Specimens exhibiting Type 3 horizontal slippage were all cast by the same concrete supplier using the same concrete proportion. With the limited test results, it is not clear what caused these specimens to exhibit that distinct behavior.

Fracture of transverse reinforcement was typically not observed in the test specimens except for Specimen RC_12#10_H4db. As can be seen in Fig. 8(f), a leg of the transverse reinforcement 16 in. (420 mm) away from the concrete base block fractured at the 135-degree seismic hook. It was observed during the second cycle of 6% target drift. Similarly, fracture of longitudinal reinforcement was typically not observed in the test specimens except for Specimen HC_12#8_H5db. As shown in Fig. 8(i), one corner

longitudinal bar on the south side fractured due to buckling rather than tension. It was observed in the second cycle of 6% target drift level when the specimen was unloaded from negative 6% target drift level (south side under compression).

Based on experimental evidence (Fig. 7 and 8), it may be concluded that specimen lateral resistances were controlled by yielding of longitudinal reinforcement and failures in all specimens were initiated by the buckling of longitudinal reinforcement regardless of spacing, type or configuration of the transverse reinforcement, followed by severe shear decay associated with the three distinct behaviors as described earlier.

Strength

Flexural—The hysteretic responses indicate that all specimens achieved the designated flexural strength before failure. The experimental-to-nominal flexural strength ratio (M_{test}/M_n) is between 1.04 and 1.17 for all test specimens as shown in Table 4, where M_{test} is the average peak flexural strength from the two loading directions and M_n is determined per ACI 318-14 with test material properties. For beam sizes

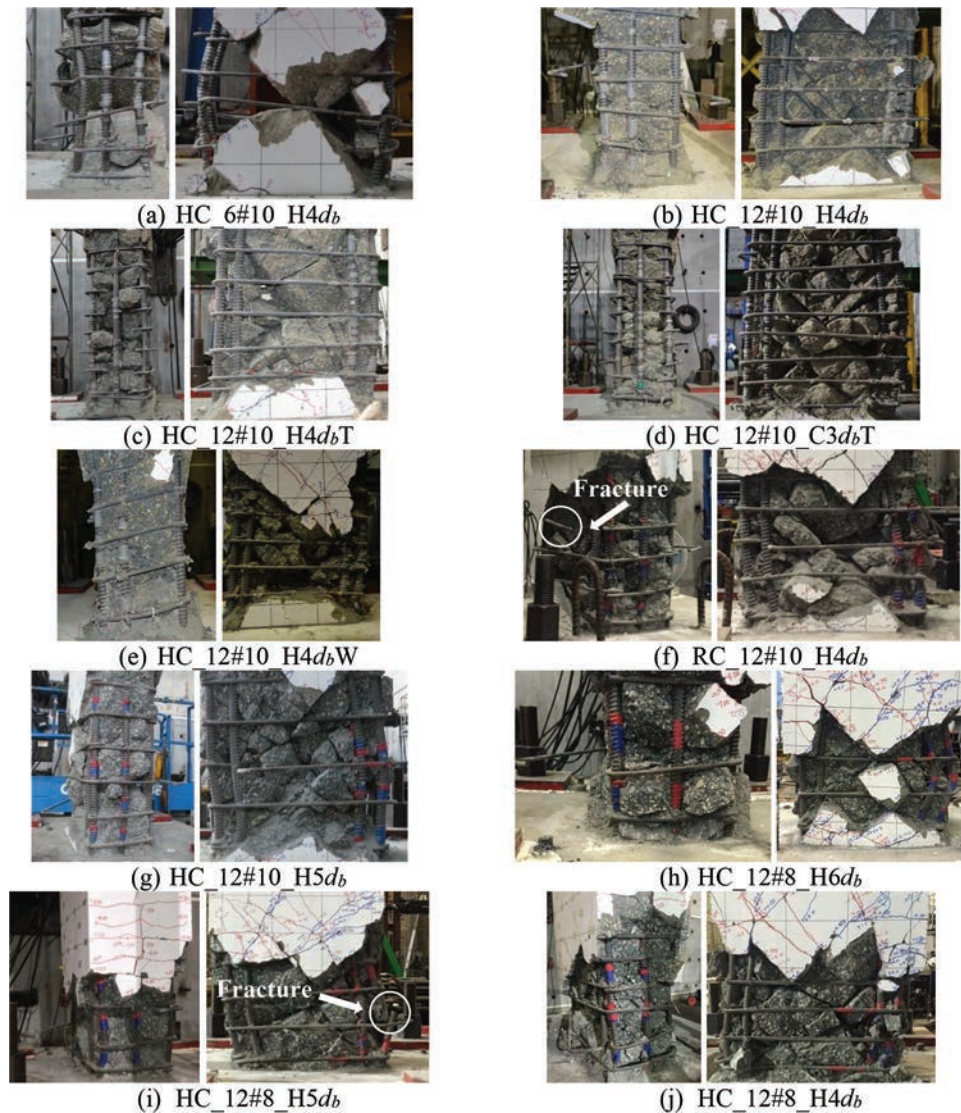


Fig. 8—Final states of test specimens.

Table 5—Observed behavior prior to failure

Specimen label	Drift level* (Cycle)	Behavior†
HC_6#10_H4db	-5.86% (2)	Type 3
HC_12#10_H4db	3.53% (3)	Type 1 and Type 3
HC_12#10_H4dbT	+3.49% (3)	Type 1
HC_12#10_C3dbT	-5.57% (1)	Type 1
HC_12#10_H4dbW	5.63% (3)	Type 1 and Type 3
RC_12#10_H4db	-5.89% (1)	Type 1 and Type 2
HC_12#10_H5db	-5.89% (1)	Type 1
HC_12#8_H6db	+5.90% (1)	Type 1
HC_12#8_H5db	-5.88% (1)	Type 1
HC_12#8_H4db	5.84% (3)	Type 2

*Drift cycle at which rapid shear decay was observed.

†Type 1 is inclined crack widths increase; Type 2 is horizontal slippage at base; and Type 3 is horizontal slippage in specimen.

similar to specimens considered in this study, nominal flexural strength estimated per ACI 318-14 using concrete cylinder strength and 1.20 specified steel yield stress ($M_{n,up}$ in Table 4) provides a satisfactory upper bound for M_{rest} .

Shear—To investigate the usable strength of high-strength transverse reinforcement for shear resistance, the average experimental lateral force interpolated at $\pm 3\%$ drift from envelope of the third loading cycle is converted to tensile stress in each leg of the hoop per ACI 318-14 and presented in column seven of Table 4. According to ACI 318-14, shear capacity of the flexural members may be determined by considering transverse reinforcement only in the region subjected to large inelastic deformation. The 3% drift from the envelope of the third loading cycle is selected as the deformation demand expected in the extreme earthquake event (maximum considered earthquake). From Table 4, the usable shear strength of high-strength transverse reinforcement ranges from 54 to 120 ksi (375 to 827 MPa). It should be noted that the usable shear strength in Specimen HC_12#10_C3dbT with Grade 60 transverse reinforcement is approximately 77 ksi (528 MPa) using the same approach.

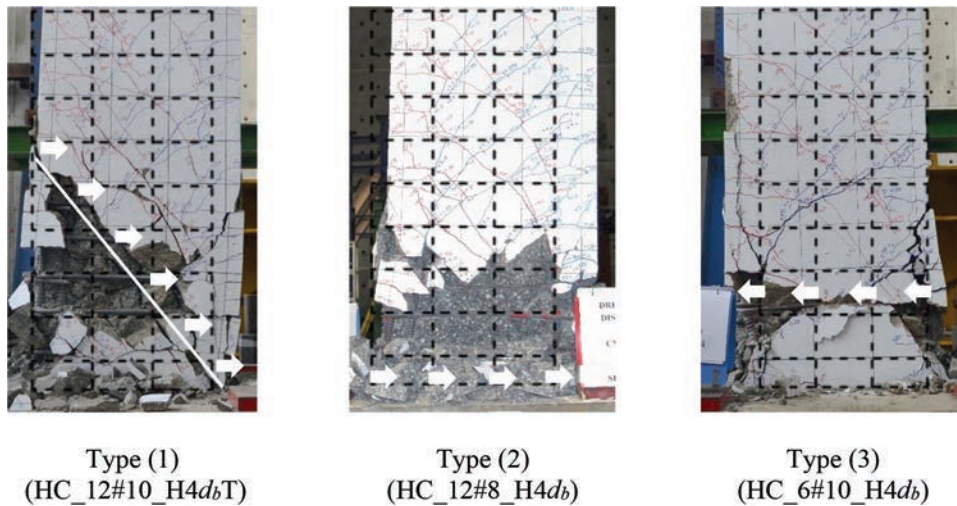


Fig. 9—Failure behavior.

The strain gauge reading on transverse reinforcement, as discussed later, supports the reported usable shear strength in Table 4.

Deformation

s/d_b —Ultimate drift ratio (d_u) of Specimen HC_12#8_H6d_b, HC_12#8_H5d_b, and HC_12#8_H4d_b is 4.8%, 5.3%, and 5.8% drift, respectively. Test results of the three specimens indicate that reducing spacing of transverse reinforcement increases deformation capacity. The 4.8% drift capacity exhibited in Specimen HC_12#8_H6d_b appears to be sufficient for special moment resisting frame (3% drift is typically expected for maximum considered earthquake). However, results of Specimen HC_12#10_H5d_b and HC_12#10_H4d_b show an opposite trend with deformation capacity of 5% and 3.5% drift, respectively. The relative low d_u in Specimen HC_12#10_H4d_b is attributed to rapid strength decay at 3.5% drift cycles (4% target drift) caused by horizontal sliding along a crack where a transverse reinforcement was provided at a distance of 11.4 in. (290 mm) away from the face of concrete base block. Whether the use of two different concrete materials in the two specimens has any influence on the overall behavior requires further research.

In Specimen HC_6#10_H4d_b, horizontal shear sliding was also observed along a transverse reinforcing bar during the 4% target drift cycles at the same height as Specimen HC_12#10_H4d_b. However, it was able to sustain the shear throughout the 4% target drift cycles and achieved deformation capacity of 5.4% drift. Shear decay due to slippage parallel to the transverse reinforcement has been reported by other researchers before (Brown and Jirsa 1971; Scribner and Wight 1980). Without intersecting the horizontal sliding plane, transverse reinforcement provides limited contribution to sustain the shear as the specimen lateral drift increases. As a result, the ultimate drift ratios d_u obtained from Specimens HC_6#10_H4d_b and HC_12#10_H4d_b may be taken as the lower-bound limit for RC beam members with equivalent design parameters.

Based on limited test results, the s/d_b not exceeding 6 appears to be enough to ensure a minimum deformation capacity of 4.8% drift for specimens having shear demand

$3.5 \sqrt{f'_c}$ (psi) ($0.29 \sqrt{f'_c}$ [MPa]) or less. For specimens with shear demand approximately $5.5 \sqrt{f'_c}$ (psi) ($0.46 \sqrt{f'_c}$ [MPa]), a minimum deformation capacity of 3.5% drift is achievable by limiting the s/d_b less than 5.

Hoop configuration—Comparing test results of Specimens HC_12#10_H4d_bW, HC_12#10_H4d_bT, and HC_12#10H4d_b, specimen strength sustained by the welded closed hoops achieved the largest d_u . Although Specimen HC_12#10_H4d_b and Specimen HC_12#10H4d_bT exhibited comparable M_{test} and d_u , shear decayed more rapidly in Specimen HC_12#10_H4d_bT during the second and third cycles of 4% target drift level. In addition, final states of the two specimens showed that seven layers of transverse reinforcement were pushed out by the end of the test in Specimens HC_12#10_H4d_bT while three layers of 135-degree hooks were pushed out in Specimen HC_12#10_H4d_b with one-piece closed hoops, as shown in Fig. 8(c) and 8(d). With transverse reinforcement spacing reduced by 25%, Specimen HC_12#10_C3d_bT failed in a nearly identical manner as Specimen HC_12#10_C4d_bT (Type 1 in Table 5), with seven layers of transverse reinforcement pushed out at the final state (Fig. 8). However, it achieved a larger deformation capacity of 4.5% drift.

Shear demand—Specimen HC_12#10_H5d_b exhibited similar failure behavior as Specimens HC_12#8_H5d_b (Type 1 in Table 5) but lower deformation capacity. A similar trend was observed in Specimens HC_12#10_H4d_b, HC_12#8_H4d_b, and HC_6#10_H4d_b, despite the three specimens failing in different manners. With the same s/d_b , it may be concluded that specimen deformation capacity increases as its shear demand decreases. However, results from Specimens HC_12#10_H4d_b and RC_12#10_H4d_b suggested that alleviating shear stress demand by increasing concrete strength was not promising to increase specimen deformation capacity. It should be reminded that strength decays in the two specimens were associated with two different manners of failure. Test results of Specimen RC_12#10_H4d_b also indicated that increasing the straight extension of 135-degree hook to prevent the hook being pushed out may not be effective because fracture was likely to occur at the bend of high-strength transverse reinforcement.

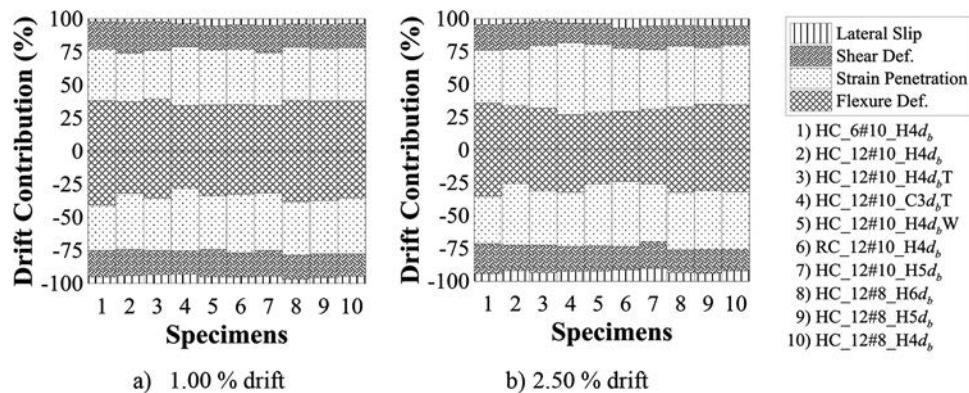


Fig. 10—Deformation components.

Deformation component—To investigate whether the composition of the deformation components varies between specimens with different design parameters, the deformation components consisting of flexural deformation, shear deformation, strain penetration and lateral slip are analyzed using the recorded marker data. Strain penetration and lateral slip represents the flexural and shear deformation, respectively, between the closely spaced markers adjacent to the wall-to-base block interface or between Row 1 and Row 2 markers in Fig. 5. Flexural deformation is estimated through accumulation of the average curvature along the height. The average curvature is obtained from curvature values of three elements in between two consecutive rows of markers. Each element is formed by four markers at the corners and its curvature value can be determined based on marker coordinates at initial and deformed stage, as presented in Fig. 5. Shear deformation is determined by subtracting flexural deformation from the overall deformation. For some specimens, markers were removed after completing the first cycle of 3% target drift due to extensive concrete cover damage. As a result, the comparison for all specimens can only be made up to approximately 2.5% drift level. As shown in Fig. 10, the drift contribution of each deformation component is determined at the first peak of each drift level and linear interpolation is used to obtain the values at 1 and 2.5% drift level. In Fig. 10, values obtained from the positive and negative loading direction are presented in the upper half and lower half of the figure, respectively.

As seen in Fig. 10, contribution of each deformation component in each specimen is more or less similar at 1 and 2.5% drift levels. The difference between each specimen is also negligible. That indicates that all specimens appear to remain structurally sound up to 2.5% drift level. Before 2.5% drift, approximately 40% of the total deformation is contributed by strain penetration and the combined shear deformation (lateral slip plus shear deformation) typically contributes approximately 25% of the total deformation.

Stiffness deterioration

When subjected to reversed loading, specimen stiffness deteriorates after each loading cycle. For each specimen, stiffness deterioration in the first cycle of each drift level is evaluated through the change of stiffness ratio at different drift levels, where stiffness ratio at a given drift level is defined as the slope of the idealized response between peak

point, shown as *m* in Fig. 11(a), divided by the slope obtained from the first cycle of 0.25% target drift. Analytical results, presented in Fig. 11(b) and 11(c), indicate that specimens with larger longitudinal reinforcement ratio exhibited better stiffness retention.

The stiffness deterioration among the three specimens having 12 No. 8 high-strength longitudinal bars is more or less similar up to 4% drift. It indicates that reducing transverse reinforcement spacing from s/d_b of 6 to 4 with usable shear strength raised from 58 to 87 ksi (402 to 600 MPa) appears to have limited influence on the rate of stiffness deterioration for specimens with shear demand of $3.5\sqrt{f'_c}$ (psi) ($0.29\sqrt{f'_c}$ [MPa]) or less.

For specimens using 12 No. 10 high-strength longitudinal bars, the trend indicates that Specimens HC_12#10_H4db and HC_12#10_H4dbT consistently exhibited slightly faster stiffness deterioration than the rest of the specimens. However, the largest difference among the specimens is typically within 5%, which may be negligible. As a result, limited test data shows the influence of using different types of hoops is not significant on stiffness retention for specimens with shear demand of approximately $5.5\sqrt{f'_c}$ (psi) ($0.46\sqrt{f'_c}$ [MPa]).

Strain gauge reading

Four strain gauges, each attached on a hoop leg, were used to measure transverse reinforcement strain at midheight of the leg in each specimen. In Specimen HC_12#10_C3dbT with conventional Grade 60 transverse reinforcement, one strain gauge with its reading and location shown in Fig. 12(a) clearly exceeded the corresponding yield strain after completion of 2% target drift. After completion of 4% target drift, strain gauges on transverse reinforcement at 9 and 16 in. (230 and 410 mm) both recorded steel strain close to 0.003 in the same specimen. It appears that results of strain gauge readings in Specimen HC_12#10_C3dbT support the reported usable shear strength of 77 ksi (528 MPa) determined at 3% drift level.

For strain gauges on high-strength transverse reinforcement, the largest recorded steel strain was typically between 0.002 and 0.004 after completion of 4% target drift depending on crack propagations and shear demand in the specimens. For example, strain gauge readings at a location approximately 28 in. (700 mm) away from the base in Specimen HC_6#10_H4db, HC_12#8_H4db, and HC_12#10_H4db is

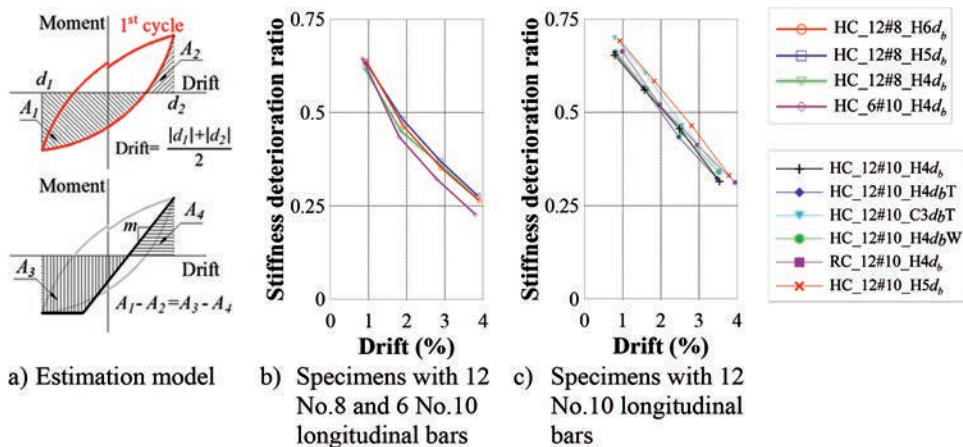


Fig. 11—Stiffness deterioration.

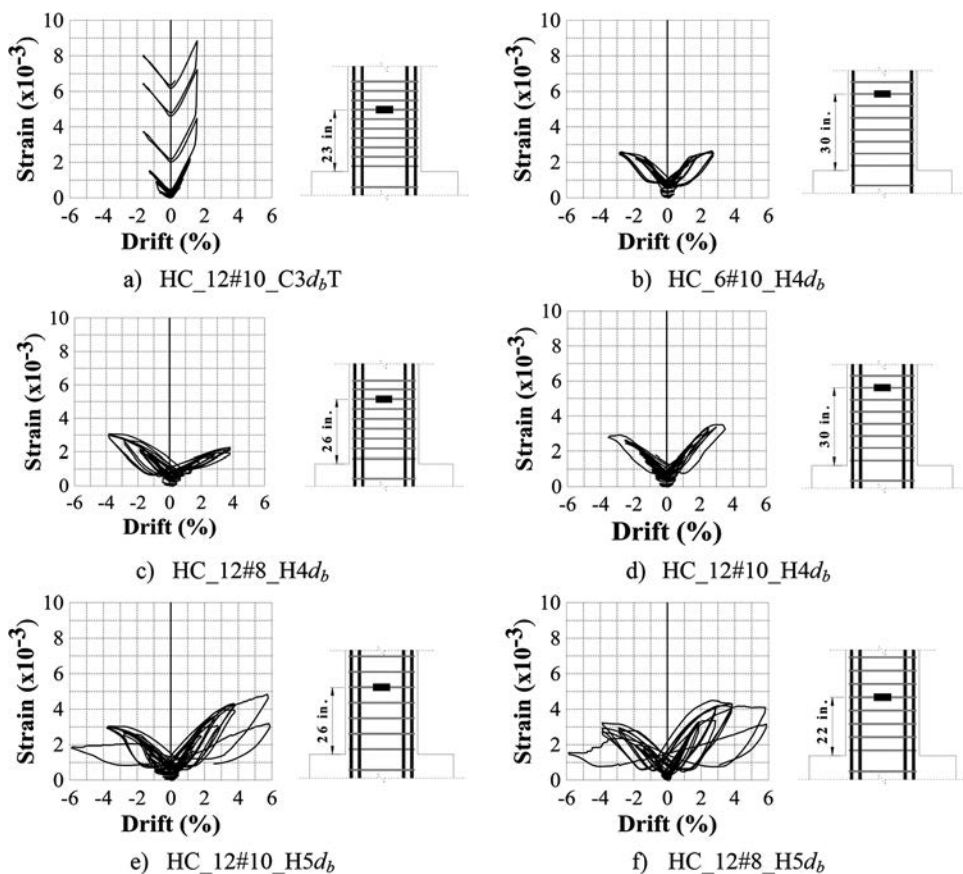


Fig. 12—Measured hoop strain. (Note: 1 in. = 25.4 mm.)

presented in Fig. 12(b), 12(c) and 12(d), respectively. Before the specimen failed or strain gauges malfunctioned, only a few high-strength transverse bars recorded values exceeding the yield strain of approximately 0.0045. Two of those were in Specimens HC_12#10_H5db and HC_12#8_H5db with hoop spacing of 5db, as shown in Fig. 12(e) and 12(f). Typically, the reported usable shear strength (Table 4) is equal to or less than those obtained from the strain gauge readings.

Strain gauges on longitudinal reinforcement, on the other hand, indicate that yielding strain of approximately 0.0035 is recorded at 28 in. (700 mm) distance away, above the face of base concrete block in most of the test specimens after completion of 3% target drift cycles. At the same stage, the marker readings in all test specimens show that

curvature is typically greater than 1.9×10^{-3} 1/in. (7.5×10^{-5} 1/mm) within bottom most marker layer (between Row 1 and Row 2 markers). A sharp curvature drop is observed above Row 2 markers. From 4 to 22 in. (100 to 550 mm) distance above the face of base concrete block, curvature gradually decreases. Above 22 in. (550 mm) distance from the base concrete block, the measured curvature is typically below 3.2×10^{-4} 1/in. (1.3×10^{-5} 1/mm).

CONCLUSIONS

Effectiveness of high-strength transverse reinforcement in cyclic behavior of high-strength RC flexural members is investigated. A total of 10 specimens were tested under displacement reversals. Primary test parameters include

spacing, configuration, and strength of transverse reinforcement. Conclusions drawn from the limited test results are provided as follows:

1. In all test specimens, peak strengths were governed by yielding of longitudinal reinforcement and failures were initiated by buckling of longitudinal reinforcement regardless of the spacing, configuration, and strength of the transverse reinforcement.

2. For beam sizes similar to specimens considered in this study, nominal flexural strength estimated per ACI 318-14 using concrete cylinder strength and 1.20 specified steel yield stress provides a satisfactory upper bound to predict specimen moment capacity.

3. The range of usable shear strength provided by the high-strength transverse reinforcement ($f_y = 115$ ksi [785 MPa]) is between 54 to 120 ksi (375 to 827 MPa).

4. For specimens using high-strength longitudinal reinforcement ($f_y = 100$ ksi [690 MPa]) with shear demand of $3.5\sqrt{f'_c}$ (psi) ($0.29\sqrt{f'_c}$ [MPa]) or less, providing transverse reinforcement with s/d_b not exceeding 6 appears to be enough to ensure a minimum deformation capacity of 4.8% drift. For specimens with shear demand of approximately $5.5\sqrt{f'_c}$ (psi) ($0.46\sqrt{f'_c}$ [MPa]), a minimum deformation capacity of 3.5% drift is achievable by limiting the s/d_b to less than 5.

5. Specimens with larger longitudinal reinforcement ratio exhibited better stiffness retention. The trend of stiffness deterioration for the specimen groups with 12 No. 8 and 12 No. 10 high-strength longitudinal bars does not appear to be significantly influenced by the hoop configuration, hoop spacing, and hoop strength considered in this study.

AUTHOR BIOS

ACI member **Leonardus S. B. Wibowo** is a PhD Candidate of civil and construction engineering at National Taiwan University of Science and Technology, Taipei, Taiwan. He received his BS in civil engineering from Universitas Brawijaya, Malang, Indonesia, and his MS in civil engineering from Institut Teknologi Sepuluh Nopember, Surabaya, Indonesia.

ACI member **Min-Yuan Cheng** is an Associate Professor in the Department of Civil and Construction Engineering at National Taiwan University of Science and Technology. He is a member of ACI Subcommittee 318-J, Joints and Connections (Structural Concrete Building Code); ACI Committee 335, Composite and Hybrid Structures; and Joint ACI-ASCE Committee 352, Joints and Connections in Monolithic Concrete Structures.

Feng-Cheng Huang is a Research Assistant at the Institute of Labor, Occupational Safety and Health, Ministry of Labor in Taiwan. He received his BS and MS from the Department of Civil and Construction Engineering at National Taiwan University of Science and Technology in 2012 and 2014, respectively.

Ting-Yu Tai is a Lecturer at National Lotung Industrial Vocational High School in Yilan, Taiwan. He received his BS and MS from the Department of Civil and Construction Engineering at National Taiwan University of Science and Technology in 2014 and 2016, respectively.

ACKNOWLEDGMENTS

The authors would like to thank the Japanese steel manufacturer Tokyo Tekko Co. for its support of this research project and for supplying the reinforcing steel. In addition, all tests were conducted in the National Center for Research on Earthquake Engineering (NCREE). The authors would also like to express their thanks to the staffs at the NCREE for their help.

NOTATION

A_1, A_2 = area between loading curve and horizontal axis (drift)
 A_3, A_4 = area between idealized loading model and horizontal axis (drift)

a	=	shear span, 83 in. (2100 mm)
b	=	width of test specimen, 16 in. (400 mm)
d	=	specimen effective depth measured from extreme compression fiber to centroid of tension flexural reinforcement
d_1, d_2	=	peak deformation (drift) in first cycle of target drift
d_b	=	diameter of smallest longitudinal reinforcement
d_u	=	ultimate drift ratio
f'_c	=	specified concrete compressive stress or average cylinder stress
f_u	=	steel coupon peak tensile stress of longitudinal reinforcement
f_{ut}	=	steel coupon peak tensile stress of transverse reinforcement
f_y	=	specified yield stress or steel coupon tested yield stress of longitudinal reinforcement
f_{yt}	=	specified yield stress or steel coupon tested yield stress of transverse reinforcement
M_n	=	nominal flexural capacity using elastic-perfectly-plastic steel response and equivalent concrete stress block
M_{n-stp}	=	predicted flexural capacity using elastic-perfectly-plastic steel response with 1.20 specified yield strength and equivalent concrete stress block with cylinder strength
M_{test}	=	average peak flexural strength from two loading directions
m	=	stiffness of idealized bilinear loading model
s	=	spacing of transverse reinforcement
V_{test}	=	average peak shear strength from two loading directions
v_u	=	shear stress demand
ϵ_{sh}	=	steel coupon tensile strain at onset of strain hardening
ϵ_{su}	=	steel coupon strain corresponding to fracture stress
Φ	=	curvature of an element
θ_{top}	=	rotation of top row of markers in an element
θ_{bottom}	=	rotation of bottom markers in an element

REFERENCES

- ACI Committee 318, 2005, "Building Code Requirements for Structural Concrete and Commentary (ACI 318-05)," American Concrete Institute, Farmington Hills, MI, 430 pp.
- ACI Committee 318, 2014, "Building Code Requirements for Structural Concrete (ACI 318-14) and Commentary," American Concrete Institute, Farmington Hills, MI, 519 pp.
- Aoyama, H., 2001, "Design of Modern High-Rise Reinforced Concrete Structures," Series of Innovation in Structures and Construction, Imperial College Press, London, UK, V. 3, 460 pp.
- ASTM A370, 2012, "Standard Test Method and Definitions for Mechanical Testing of Steel Products," ASTM International, West Conshohocken, PA, 48 pp.
- Brown, R. H., and Jirsa, J. O., 1971, "Reinforced Concrete Beams under Load Reversals," *ACI Journal Proceedings*, V. 68, No. 5, May, pp. 380-390.
- Cheng, M.-Y., and Giduquio, M. B., 2014, "Cyclic Behavior of Reinforced Concrete Flexural Members Using High-Strength Flexural Reinforcement," *ACI Structural Journal*, V. 111, No. 4, Jul.-Aug., pp. 893-902.
- Falkner, H.; Gerritzen, D.; Jungwirth, D.; and Sparowitz, L., 2008, "The New Reinforcement System; Compression Members with SAS 670 High-Strength Reinforcement Steel—Part I: Development, Testing, Design and Construction," *Beton- und Stahlbetonbau*, Ernst & Sohn, Berlin, Germany, 31 pp.
- Giduquio, M. B.; Cheng, M.-Y.; and Wibowo, L. S. B., 2015, "High-Strength Flexural Reinforcement in Reinforced Concrete Flexural Members under Monotonic Loading," *ACI Structural Journal*, V. 112, No. 6, Nov.-Dec., pp. 793-804.
- Lee, J.-Y.; Choi, I.-J.; and Kim, S.-W., 2011, "Shear Behavior of Reinforced Concrete Beams with High-Strength Stirrups," *ACI Structural Journal*, V. 108, No. 5, Sep.-Oct., pp. 620-629.
- NIST GCR 14-917-30, 2014, "Use of High-Strength Reinforcement in Earthquake-Resistant Concrete Structures," NEHRP Consultant Joint Venture, Redwood City, CA, 231 pp.
- Rautenberg, J. M., 2011, "Drift Capacity of Concrete Columns Reinforced with High-Strength Steel," PhD dissertation, Purdue University, West Lafayette, IN, May, 263 pp.
- Scribner, C. F., and Wight, J. K., 1980, "Strength Decay in R/C Beams Under Load Reversals," *Journal of the Structural Division*, ASCE, V. ST4, April, pp. 861-876.
- Sumpter, M. S.; Rizkalla, S. H.; and Zia, P., 2009, "Behavior of High-Performance Steel as Shear Reinforcement for Concrete Beams," *ACI Structural Journal*, V. 106, No. 2, Mar.-Apr., pp. 171-177.
- Tavallali, H.; Lepage, A.; Rautenberg, J. M.; and Pujol, S., 2014, "Concrete Beams Reinforced with High-Strength Steel Subjected to Displacement Reversals," *ACI Structural Journal*, V. 111, No. 5, Sep.-Oct., pp. 1037-1048.